

Prediction of large gap flat Chern band in a two-dimensional metal-organic framework

Ninghai Su, Wei Jiang, Zhengfei Wang, and Feng Liu

Citation: *Appl. Phys. Lett.* **112**, 033301 (2018);

View online: <https://doi.org/10.1063/1.5017956>

View Table of Contents: <http://aip.scitation.org/toc/apl/112/3>

Published by the [American Institute of Physics](#)

Articles you may be interested in

[Topological optical isolator based on polariton graphene](#)

Applied Physics Letters **112**, 031106 (2018); 10.1063/1.5018902

[Broadband nonlinear optical response of monolayer MoSe₂ under ultrafast excitation](#)

Applied Physics Letters **112**, 031108 (2018); 10.1063/1.5010060

[Manipulation of electron transport in graphene by nanopatterned electrostatic potential on an electret](#)

Applied Physics Letters **112**, 033102 (2018); 10.1063/1.5006226

[The interplay between excitons and trions in a monolayer of MoSe₂](#)

Applied Physics Letters **112**, 031107 (2018); 10.1063/1.5019177

[Leaky electronic states for photovoltaic photodetectors based on asymmetric superlattices](#)

Applied Physics Letters **112**, 033503 (2018); 10.1063/1.5006464

[Photo-conductive detection of continuous THz waves via manipulated ultrafast process in nanostructures](#)

Applied Physics Letters **112**, 031102 (2018); 10.1063/1.5008790



Scilight

Sharp, quick summaries **illuminating**
the latest physics research

Sign up for **FREE!**

AIP
Publishing

Prediction of large gap flat Chern band in a two-dimensional metal-organic framework

Ninghai Su,¹ Wei Jiang,¹ Zhengfei Wang,² and Feng Liu^{1,a)}

¹Department of Materials Science and Engineering, University of Utah, Salt Lake City, Utah 84112, USA

²Hefei National Laboratory for Physical Sciences at the Microscale, University of Science and Technology of China, Hefei, Anhui 230026, China

(Received 1 December 2017; accepted 29 December 2017; published online 18 January 2018)

Systems with a flat Chern band have been extensively studied for their potential to realize high-temperature fractional quantum Hall states. To experimentally observe the quantum transport properties, a sizable topological gap is highly necessary. Here, taking advantage of the high tunability of two-dimensional (2D) metal-organic frameworks (MOFs), whose crystal structures can be easily tuned using different metal atoms and molecular ligands, we propose a design of a 2D MOF [Tl₂(C₆H₄)₃, Tl₂Ph₃] showing nontrivial topological states with an extremely large gap in both the nearly flat Chern band and the Dirac bands. By coordinating π -conjugated thallium ions and benzene rings, crystalline Tl₂Ph₃ can be formed with Tl and Ph constructing honeycomb and kagome lattices, respectively. The $p_{x,y}$ orbitals of Tl on the honeycomb lattice form ideal p_{xy} four-bands, through which a flat Chern band with a spin-orbit coupling (SOC) gap around 140 meV evolves below the Fermi level. This is the largest SOC gap among all the theoretically proposed organic topological insulators so far. *Published by AIP Publishing.* <https://doi.org/10.1063/1.5017956>

The recently proposed flat Chern band (FCB) in two-dimensional (2D) structures^{1–3} is featured with both exotic band dispersion and topological order, which are signatures of graphene^{4,5} and topological insulators (TIs),^{6,7} respectively. With a smaller bandwidth than both the interaction energy scale and the energy gap between the FCB and its neighboring bands, the kinetic energy of carriers in the FCB is strongly suppressed, which gives rise to exotic topological states^{8–11} because any infinitely small interaction can be significant. Distinguished from other “normal” narrow/flat bands, such as the surface dangling bond or the bulk defect state in semiconductors or the localized state in heavy fermion compounds, which are all topologically trivial, FCB is topologically nontrivial with a well-defined nontrivial Chern number. A flat band with a nontrivial Chern variant is a consequence from a well-balanced effect of lattice hopping, spin-orbit coupling (SOC), and ferromagnetism. Because of the rigorous criteria, except for the theoretical models proposed in Refs. 1–3, no real material has been reported until very recently when the concept of organic topological insulators (OTIs) was proposed.^{12,13} Based on the same theme, two 2D organometallic frameworks were delicately designed to realize FCB, i.e., indium-phenylene and gold-phenalenyl organometallic frameworks.^{14,15} However, due to the weak SOC of In and Au ions, the SOC gap is fairly small, which is around 30 and 8 meV for In- and Au-based metal-organic framework (MOF), respectively. For its potential applications in electronics and spintronics at room temperature, a larger energy gap is highly desirable. In this work, we present a first-principles design to enlarge the SOC gap of a 2D MOF with nontrivial FCB by replacing indium with thallium, which has a stronger SOC while maintaining the symmetry and topology of the MOF system.

Our first-principles calculations are carried out within the framework of the Perdew-Burke-Ernzerhof generalized gradient approximation using VASP.¹⁶ All the calculations are performed with a plane-wave cutoff of 600 eV on the $11 \times 11 \times 1$ Monkhorst-Pack k-point mesh. The vacuum layer is chosen to be 20 Å thick to ensure decoupling between neighboring slabs. During structural relaxation, all atoms are relaxed until the forces are smaller than 0.01 eV/Å.

Figure 1 shows the optimized 2D atomic structure of the Tl₂Ph₃ lattice, which adopts a mixed honeycomb and kagome lattice by binding p -orbital heavy elements (Tl) with organic ligands (paraphenylene groups). The dashed yellow lines show the unit cell with a lattice constant of 12.70 Å, which contains two Tl ions forming a honeycomb lattice and three paraphenylene groups constructing a kagome lattice. It is worth noting that the Tl₂Ph₃ lattice resembles the already

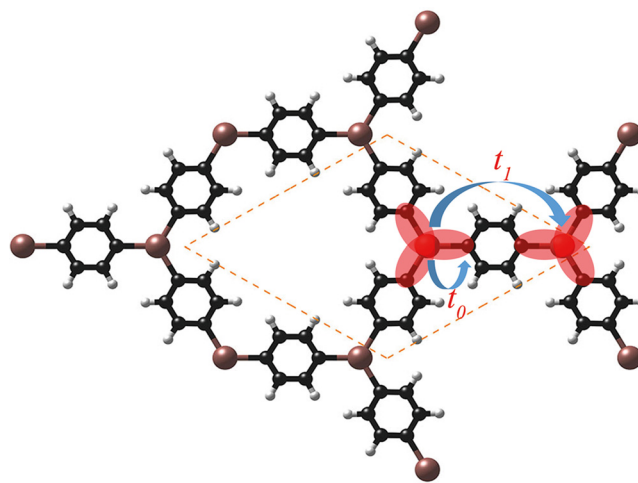


FIG. 1. Atomic structure of the Tl₂Ph₃ lattice. The dashed orange lines denote the unit cell.

^{a)}Electronic mail: fliu@eng.utah.edu

synthesized organic framework with only Tl ions replaced by boroxine rings.^{17,18}

Figure 2(b) shows both the band structure on a path intersecting several high symmetry points as labeled in Fig. 2(a) and the atomic-orbital projected density of states (APDOS) of the Tl_2Ph_3 lattice without SOC. The band structure indicates that the Tl_2Ph_3 lattice is a nonmagnetic insulator with a bandgap of about 2.5 eV. The four signature bands indicated by Ref. 14 can be clearly seen in the valence zone near the Fermi level, consisting of two nearly flat bands sandwiching two dispersive bands with a Dirac cone formed at the K point. The top and bottom flat bands are nearly flat in the whole Brillouin zone with narrow bandwidths of 12 meV and 33 meV, respectively. The flat bands and the dispersive bands touch each other at the Γ point. Moreover, there are also six bands within the energy range between the top and bottom flat bands, which come from the p_z orbitals of C and Tl atoms. Comparing Fig. 2(b) with the results shown in Ref. 14, the most significant difference is that the Dirac cone at the K point formed by the two dispersive bands is now well separated from the six p_z bands. Considering the similarity between our material and that in Ref. 14, we expect that Tl_2Ph_3 will also be topologically nontrivial with SOC gaps opening at both the Dirac cone and the Γ point between flat and Dirac bands.

Then, we include SOC in the first-principles calculation, and the results are shown in Fig. 2(c). Comparing Fig. 2(c) with Fig. 2(b), the degenerate Γ and K points of the four bands are now split, which results in finite gaps at these points. The bandgap of the Dirac band is $\Delta^{23} = 255$ meV, while the direct and indirect bandgaps between the top flat band and the top branch of the dispersive bands are $\Delta_{dir}^{12} = 284$ meV and $\Delta_{ind}^{12} = 143$ meV, respectively. The separation between the top and bottom flat bands is $\Delta_{14} = 1.3$ eV. Also, in the presence of SOC, the bandwidth of the top and bottom flat bands increases

from 12 meV and 33 meV to 140 meV and 89 meV, respectively. We note that all the bands are spin degenerate due to the time-reversal and inversion symmetry, and the system remains intrinsically a band insulator.

Because of the large DOS of the flat band around the Fermi level, with specific electron filling, even an arbitrarily small Coulomb interaction will drive the system into a ferromagnetic ground state based on the Stoner criterion.^{19,20} Thus, we performed a computational experiment by introducing one hole into the unit cell, while maintaining the charge neutrality with a compensating homogenous background charge, through which we can easily separate the spin-up and spin-down bands. It is worth mentioning that the MOF system can be doped using gating experiments, the redox control method,^{21–23} or a radical molecule.¹⁵ Figure 2(d) shows the band structure of the hole-doped Tl_2Ph_3 lattice. The degenerate spin-up and spin-down components are split, with the Fermi level lying in between the two spin-polarized flat bands. The total energy of the Tl_2Ph_3 lattice in the ferromagnetic ground state is found to be 30 meV lower than that in the spin-unpolarized state, and the antiferromagnetic state is found unstable. The ferromagnetic spins are mainly localized in the Tl honeycomb lattice. As discussed in Ref. 14, the external Zeeman field can provide additional stabilization to the ferromagnetic Tl_2Ph_3 lattice.

As shown in Fig. 2(d), the spin splitting U is about 228 meV, which represents the strength of the on-site Coulomb interaction. We summarize in Table I several key energy scales associated with the FCB of the Tl_2Ph_3 lattice and compare them with the results of the In_2Ph_3 studied in Ref. 14. Because of the strong SOC effect of the heavy metal element Tl, we notice that the SOC gaps at both the Dirac point and the Γ point between flat and Dirac bands in the Tl_2Ph_3 are much larger than that in In_2Ph_3 . The SOC gap (255 meV) at the Dirac point is much larger than most of the TIs, and a TI state will evolve with suitable electron doping.

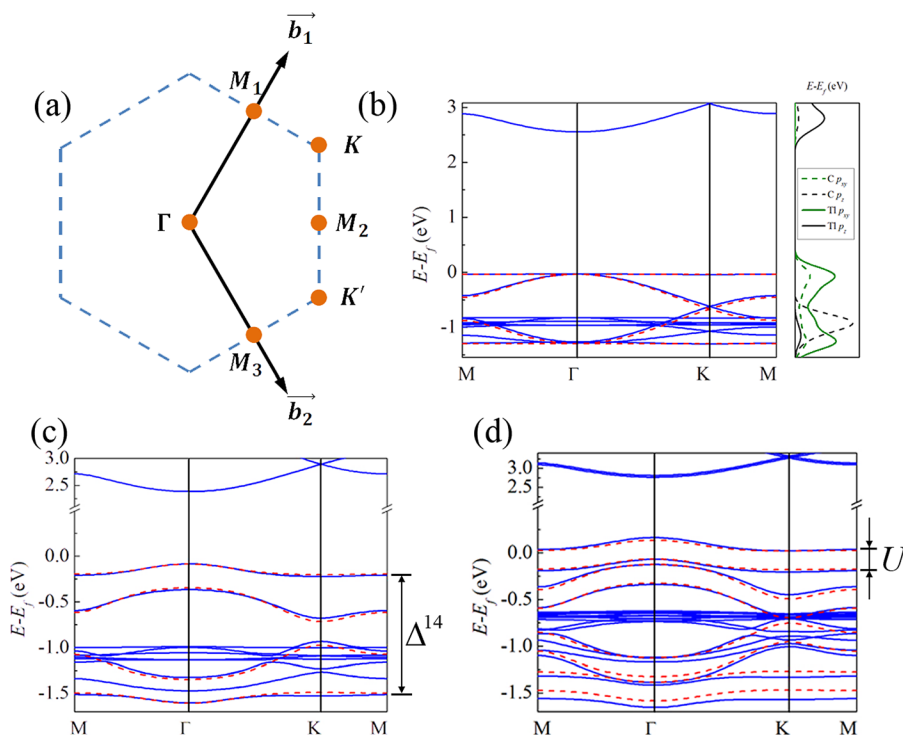


FIG. 2. Band structure of the Tl_2Ph_3 lattice. (a) The first Brillouin zone and high symmetry points. (b) Band structure and atomic-orbital projected DOS of the Tl_2Ph_3 lattice without SOC. (c) Band structure with SOC. (d) Band structure with SOC and one hole doped per unit cell. The blue solid lines represent our first principles results, and the red dashed lines are results from the TB model [Eq. (9)] with parameters: (a) $t_1 = 0.63$; (b) $t_1 = 0.63$, $\lambda = 0.05$ eV; (c) $t_1 = 0.63$ eV, $\lambda = 0.13$ eV, and $M = 0.1$ eV.

TABLE I. Comparison of some energy scales between Ti_2Ph_3 and In_2Ph_3 (Ref. 14) lattices.

Property	Symbol	Ti_2Ph_3	In_2Ph_3 (Ref. 14)
Bandwidth	W	140 meV [Fig. 3(a)]	60 meV
Spin splitting	U	228 meV [Fig. 2(d)]	100 meV
Energy gap	Δ_{dir}^{12}	284 meV [Fig. 3(a)]	90 meV
	Δ_{ind}^{12}	143 meV [Fig. 3(a)]	30 meV
	Δ^{23}	255 meV [Fig. 3(a)]	90 meV
	Δ^{14}	1.3 eV [Fig. 2(c)]	1.4 eV

More importantly, in our Ti_2Ph_3 system, the direct bandgap Δ_{dir}^{12} (284 meV) is much larger than the flat band width W (140 meV), while Δ_{dir}^{12} (90 meV) is only slightly larger than the bandwidth of the flat band (60 meV) in the In_2Ph_3 system. The larger this energy scale difference, the more likely the topological properties associated with the FCB, especially the fractional quantum Hall effect to be experimentally measured.¹ It is worth mentioning that these are the largest SOC gaps among all the organic TIs (OTIs) proposed so far,^{12–15,24–29} which are even comparable to those of large-gap inorganic TIs.^{30–33}

Further, to study its topological properties, we will first check the edge states of a semi-infinite Ti_2Ph_3 lattice by calculating the momentum-resolved edge DOS as the number of chiral edge modes circulating around the boundary is an important signature of the nontrivial flat band. We calculated the edge states by using the Wannier90 package,³⁴ in which a tight-binding (TB) Hamiltonian in the basis of the maximally localized Wannier functions (MLWFs) is fitted to the first-principles band structures. Using these MLWFs, the edge Green's function of the semi-infinite lattice is constructed using the recursive method,³⁵ and the local density of states (LDOS) of the edge is calculated. This method provides a direct connectivity between the edge states and the bulk states. The LDOS of a semi-infinite Ti_2Ph_3 is shown in Figs. 3(b) and 3(c) for spin-up and spin-down components, respectively, where one can clearly see the nontrivial topological edge states that connect the bulk states and form a 1D Dirac cone in both SOC gaps (Δ^{12} and Δ^{23}).

Then, to further confirm the nontrivial topology of the Ti_2Ph_3 lattice, we have calculated the Chern number (C) and spin Chern number (C^s) using the Kubo formula^{36,37} as follows:

$$C = \frac{1}{2\pi} \int_{BZ} d^2\vec{k} \Omega(\vec{k}), \quad (1)$$

$$\Omega(\vec{k}) = \sum_n f_n \Omega_n(\vec{k}), \quad (2)$$

$$\Omega_n(\vec{k}) = - \sum_{n' \neq n} 2\text{Im} \frac{\langle \Psi_{nk} | \nu_x | \Psi_{n'k} \rangle \langle \Psi_{n'k} | \nu_y | \Psi_{nk} \rangle}{(\varepsilon_{n'k} - \varepsilon_{nk})^2}, \quad (3)$$

$$C^s = \frac{1}{2\pi} \int_{BZ} d^2\vec{k} \Omega^s(\vec{k}), \quad (4)$$

$$\Omega^s(\vec{k}) = \sum_n f_n \Omega_n^s(\vec{k}), \quad (5)$$

$$\Omega_n^s(\vec{k}) = - \sum_{n' \neq n} 2\text{Im} \frac{\langle \Psi_{nk} | j_x | \Psi_{n'k} \rangle \langle \Psi_{n'k} | \nu_y | \Psi_{nk} \rangle}{(\varepsilon_{n'k} - \varepsilon_{nk})^2}, \quad (6)$$

where n is the band index, Ψ_{nk} are the eigenstate of eigenvalue ε_{nk} of band n , f_n is the Fermi distribution function, $\nu_{x/y}$ is the velocity operator, j_x is the spin current operator defined as $(s_z \nu_x + \nu_x s_z)/2$, and s_z is the spin operator. The Chern number and spin Chern number are defined as

$$C = C_\uparrow + C_\downarrow \quad C^s = \frac{1}{2}(C_\uparrow - C_\downarrow). \quad (7)$$

From Eqs. (1)–(7), the Chern numbers of each band with different spins are calculated, as marked in Fig. 3(a). For both spins, the top flat band and the lower Dirac band have a non-zero Chern number (± 1), while the upper Dirac band has a zero Chern number. As a consequence, within the SOC gap of Δ^{12} and Δ^{23} , the Chern number is zero, but the spin Chern number is -1 , which demonstrates that the Ti_2Ph_3 lattice is topologically nontrivial. Moreover, the spin Berry curvatures for both the flat and Dirac bands are calculated, as shown in Figs. 4(b) and 4(c), which further confirm its topological nontriviality. The coexistence of two TI states, one from the Dirac band and the other from the topmost flat band, at different energies can manifest in the transport measurement. The spin Hall conductance can be obtained from the spin Chern number as

$$\sigma_{xy}^{SH} = \frac{e}{4\pi} (C_\uparrow - C_\downarrow). \quad (8)$$

Figure 4(a) shows the calculated spin Hall conductance as a function of energy using the first-principles method, which has a quantized value ($-2e/4\pi$) within the energy window of both SOC gaps.

The four bands of the Ti_2Ph_3 lattice can be described by using the p_{xy} four-band TB model,¹⁴ from which we can obtain a better understanding about the FCB in the Ti_2Ph_3

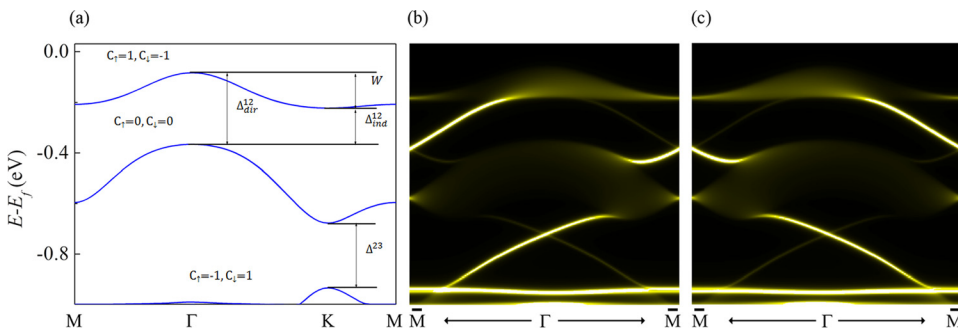


FIG. 3. Evidences of topological states in the Ti_2Ph_3 lattice. (a) Band structure of the Ti_2Ph_3 lattice near the Fermi level. (b) and (c) The semi-infinite edge states for the spin-up and spin-down components, respectively. Overlapping these two figures will show the 1D edge Dirac band in both SOC gaps.

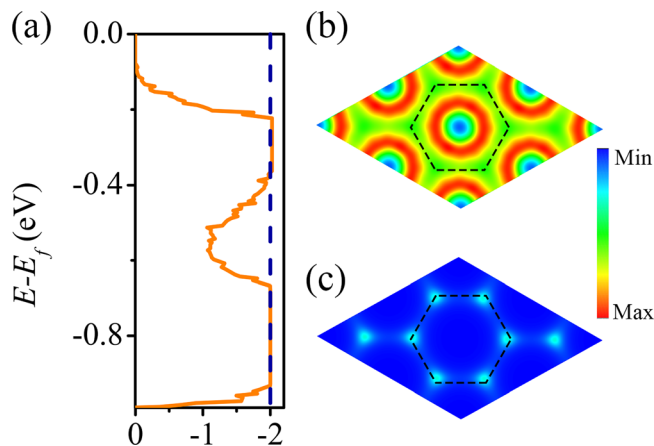


FIG. 4. Hall conductance and the Berry phase in the Tl_2Ph_3 lattice. (a) Quantized spin Hall conductance within the energy window of the two SOC gaps. (b) and (c) Spin Berry curvatures in the reciprocal space for flat (b) and Dirac bands (c). The dashed line marks the first Brillouin zone.

lattice. The corresponding effective Hamiltonian can be expressed as follows:

$$H = -t_1 \begin{pmatrix} 0 & 0 & V_{xx} & V_{xy} \\ 0 & 0 & V_{xy} & V_{yy} \\ V_{xx}^* & V_{xy}^* & 0 & 0 \\ V_{xy}^* & V_{yy}^* & 0 & 0 \end{pmatrix} + \sigma_z \lambda \begin{pmatrix} 0 & -i & 0 & 0 \\ i & 0 & 0 & 0 \\ 0 & 0 & 0 & -i \\ 0 & 0 & -i & 0 \end{pmatrix} + \sigma_z M, \quad (9)$$

in which $\sigma_z = \pm 1$ is the spin eigenvalue, $V_{xx} = \frac{1}{2}(1 + e^{ik \cdot \mathbf{a}_1})$, $V_{xy} = \frac{\sqrt{3}}{6}(1 - e^{ik \cdot \mathbf{a}_1})$, and $V_{yy} = \frac{1}{\sqrt{6}}(1 + e^{ik \cdot \mathbf{a}_1} + 4e^{ik \cdot \mathbf{a}_2})$; $\mathbf{a}_{1,2}$ is the lattice vector. There are three parameters in the model: the next-nearest-neighbor hopping parameter t_1 , the SOC strength λ , and the exchange energy for spin splitting M that equals $U/2$, where U denotes the Coulomb interaction. By fitting the three parameters to the first-principles calculated results, the dispersion of the four p_{xy} bands can be well reproduced, as is shown in Figs. 2(b)–2(d). The TB model analysis indicates that the SOC gaps (Δ^{12} and Δ^{23}) in the Tl_2Ph_3 lattice are opened due to the intrinsic SOC of the p_{xy} orbitals of TI atoms, given the inversion lattice symmetry that excludes the Rashba SOC effect.

In conclusion, we predicted the existence of a flat Chern band around the Fermi level in a 2D MOF. Our study indicates that the Tl_2Ph_3 lattice has the largest SOC gap among all the OTIs proposed so far, which is comparable to that of typical large gap inorganic TIs. The flat and Dirac bands mainly originate from p_{xy} orbitals of TI atoms with large SOC, resulting in the large SOC gap. By doping one hole per unit cell, FCB can be realized leading to the possible fractional quantum anomalous Hall state. Our prediction is valuable in guiding the experimental search for large gap OTIs, and we note that there are still many difficult steps to be completed to perform quantum Hall experiments on this MOF system.

N. Su and F. Liu are supported by U.S. DOE-BES (Grant No. DE-FG02-04ER46148). W. Jiang is supported by

the National Science Foundation-Material Research Science & Engineering Center (NSF-MRSEC Grant No. DMR-1121252). We also thank the CHPC at the University of Utah and DOE-NERSC for providing the computing resources.

- ¹E. Tang, J.-W. Mei, and X.-G. Wen, “High-temperature fractional quantum Hall states,” *Phys. Rev. Lett.* **106**, 236802 (2011).
- ²K. Sun, Z. Gu, H. Katsura, and S. Das Sarma, “Nearly flatbands with non-trivial topology,” *Phys. Rev. Lett.* **106**, 236803 (2011).
- ³T. Neupert, L. Santos, C. Chamon, and C. Mudry, “Fractional quantum Hall states at zero magnetic field,” *Phys. Rev. Lett.* **106**, 236804 (2011).
- ⁴A. K. Geim, “Nobel lecture: Random walk to graphene,” *Rev. Mod. Phys.* **83**, 851–862 (2011).
- ⁵K. S. Novoselov, “Nobel lecture: Graphene: Materials in the flatland,” *Rev. Mod. Phys.* **83**, 837–849 (2011).
- ⁶X.-L. Qi and S.-C. Zhang, “Topological insulators and superconductors,” *Rev. Mod. Phys.* **83**, 1057–1110 (2011).
- ⁷M. Z. Hasan and C. L. Kane, “Colloquium: Topological insulators,” *Rev. Mod. Phys.* **82**, 3045–3067 (2010).
- ⁸D. N. Sheng, Z.-C. Gu, K. Sun, and L. Sheng, “Fractional quantum Hall effect in the absence of Landau levels,” *Nat. Commun.* **2**, 389 (2011).
- ⁹J. W. F. Venderbos, M. Daghofer, and J. van den Brink, “Narrowing of topological bands due to electronic orbital degrees of freedom,” *Phys. Rev. Lett.* **107**, 116401 (2011).
- ¹⁰Y.-F. Wang, Z.-C. Gu, C.-D. Gong, and D. N. Sheng, “Fractional quantum Hall effect of hard-core bosons in topological flat bands,” *Phys. Rev. Lett.* **107**, 146803 (2011).
- ¹¹W. Jiang, Z. Liu, J.-W. Mei, B. Cui, and F. Liu, “Tunable Bi-frustrated electron spin and charge states in a Cu-hexaaminobenzene framework,” e-print [arXiv:1711.09931](https://arxiv.org/abs/1711.09931) [cond-mat.str-el].
- ¹²Z. F. Wang, Z. Liu, and F. Liu, “Organic topological insulators in organometallic lattices,” *Nat. Commun.* **4**, 1471 (2013).
- ¹³Z. F. Wang, Z. Liu, and F. Liu, “Quantum anomalous Hall effect in 2d organic topological insulators,” *Phys. Rev. Lett.* **110**, 196801 (2013).
- ¹⁴Z. Liu, Z.-F. Wang, J.-W. Mei, Y.-S. Wu, and F. Liu, “Flat Chern band in a two-dimensional organometallic framework,” *Phys. Rev. Lett.* **110**, 106804 (2013).
- ¹⁵M. G. Yamada, T. Soejima, N. Tsuji, D. Hirai, M. Dincă, and H. Aoki, “First-principles design of a half-filled flat band of the kagome lattice in two-dimensional metal-organic frameworks,” *Phys. Rev. B* **94**, 081102 (2016).
- ¹⁶G. Kresse and J. Hafner, “*Ab initio* molecular dynamics for liquid metals,” *Phys. Rev. B* **47**, 558–561 (1993).
- ¹⁷O. Ourdjini, R. Pawlak, M. Abel, S. Clair, L. Chen, N. Bergeon, M. Sassi, V. Oison, J.-M. Debierre, R. Coratger, and L. Porte, “Substrate-mediated ordering and defect analysis of a surface covalent organic framework,” *Phys. Rev. B* **84**, 125421 (2011).
- ¹⁸N. A. A. Zwaneveld, R. Pawlak, M. Abel, D. Catalin, D. Gimes, D. Bertin, and L. Porte, “Organized formation of 2d extended covalent organic frameworks at surfaces,” *J. Am. Chem. Soc.* **130**, 6678–6679 (2008).
- ¹⁹A. Mielke, “Ferromagnetic ground states for the Hubbard model on line graphs,” *J. Phys. A: Math. Gen.* **24**, L73 (1991).
- ²⁰A. Mielke, “Ferromagnetism in the Hubbard model on line graphs and further considerations,” *J. Phys. A: Math. Gen.* **24**, 3311 (1991).
- ²¹T. Kambe, R. Sakamoto, T. Kusamoto, T. Pal, N. Fukui, K. Hoshiko, T. Shimojima, Z. Wang, T. Hirahara, K. Ishizaka, S. Hasegawa, F. Liu, and H. Nishihara, “Redox control and high conductivity of nickel bis(dithiolenes) complex Π -nanosheet: A potential organic two-dimensional topological insulator,” *J. Am. Chem. Soc.* **136**, 14357–14360 (2014).
- ²²X. Sun, K.-H. Wu, R. Sakamoto, T. Kusamoto, H. Maeda, X. Ni, W. Jiang, F. Liu, S. Sasaki, H. Masunaga, and H. Nishihara, “Bis(aminothiolato)nickel nanosheet as a redox switch for conductivity and an electrocatalyst for the hydrogen evolution reaction,” *Chem. Sci.* **8**, 8078–8085 (2017).
- ²³E. J. H. Phua, K.-H. Wu, K. Wada, T. Kusamoto, H. Maeda, J. Cao, R. Sakamoto, H. Masunaga, S. Sasaki, J.-W. Mei, W. Jiang, F. Liu, and H. Nishihara, “Oxidation-promoted interfacial synthesis of redox-active bis(diimino)nickel nanosheet,” *Chem. Lett.* **47**, 126–129 (2018).
- ²⁴Z. F. Wang, N. Su, and F. Liu, “Prediction of a two-dimensional organic topological insulator,” *Nano Lett.* **13**, 2842–2845 (2013).
- ²⁵X. Zhang and M. Zhao, “Robust half-metallicity and topological aspects in two-dimensional Cu-TPyB,” *Sci. Rep.* **5**, 14098 (2015).

- ²⁶L. Wei, X. Zhang, and M. Zhao, "Spin-polarized Dirac cones and topological nontriviality in a metal-organic framework $\text{Ni}_2\text{C}_{24}\text{S}_6\text{H}_{12}$," *Phys. Chem. Chem. Phys.* **18**, 8059–8064 (2016).
- ²⁷X. Zhang, Z. Wang, M. Zhao, and F. Liu, "Tunable topological states in electron-doped HTT-Pt," *Phys. Rev. B* **93**, 165401 (2016).
- ²⁸L. Dong, Y. Kim, D. Er, A. M. Rappe, and V. B. Shenoy, "Two-dimensional π -conjugated covalent-organic frameworks as quantum anomalous Hall topological insulators," *Phys. Rev. Lett.* **116**, 096601 (2016).
- ²⁹Z. F. Wang, K.-H. Jin, and F. Liu, "Computational design of two-dimensional topological materials," *Wiley Interdiscip. Rev.: Comput. Mol. Sci.* **7**, e1304 (2017).
- ³⁰Y. Xia, D. Qian, D. Hsieh, L. Wray, A. Pal, H. Lin, A. Bansil, D. Grauer, Y. S. Hor, R. J. Cava, and M. Z. Hasan, "Observation of a large-gap topological-insulator class with a single Dirac cone on the surface," *Nat. Phys.* **5**, 398 (2009).
- ³¹Y. Xu, B. Yan, H.-J. Zhang, J. Wang, G. Xu, P. Tang, W. Duan, and S.-C. Zhang, "Large-gap quantum spin Hall insulators in tin films," *Phys. Rev. Lett.* **111**, 136804 (2013).
- ³²C. Si, J. Liu, Y. Xu, J. Wu, B.-L. Gu, and W. Duan, "Functionalized germanene as a prototype of large-gap two-dimensional topological insulators," *Phys. Rev. B* **89**, 115429 (2014).
- ³³H. Weng, X. Dai, and Z. Fang, "Transition-metal pentatelluride ZrTe_5 and HfTe_5 : A paradigm for large-gap quantum spin Hall insulators," *Phys. Rev. X* **4**, 011002 (2014).
- ³⁴A. A. Mostofi, J. R. Yates, Y.-S. Lee, I. Souza, D. Vanderbilt, and N. Marzari, "Wannier90: A tool for obtaining maximally-localised wannier functions," *Comput. Phys. Commun.* **178**, 685–699 (2008).
- ³⁵M. P. L. Sancho, J. M. L. Sancho, J. M. L. Sancho, and J. Rubio, "Highly convergent schemes for the calculation of bulk and surface green functions," *J. Phys. F: Met. Phys.* **15**, 851 (1985).
- ³⁶Y. Yao and Z. Fang, "Sign changes of intrinsic spin Hall effect in semiconductors and simple metals: First-principles calculations," *Phys. Rev. Lett.* **95**, 156601 (2005).
- ³⁷Y. Yao, L. Kleinman, A. H. MacDonald, J. Sinova, T. Jungwirth, D.-S. Wang, E. Wang, and Q. Niu, "First principles calculation of anomalous Hall conductivity in ferromagnetic bcc Fe," *Phys. Rev. Lett.* **92**, 037204 (2004).